In-silico reverse docking and _in-vitro_ studies identified curcumin, 18α-glycyrrhetinic acid, rosmarinic acid, and quercetin as inhibitors of α-glucosidase and pancreatic α-amylase and lipid accumulation in HepG2 cells, important type 2 diabetes targets

Kadima Samuel TSHIYOYO[1], Megan Jean BESTER[2], June C. SEREM[2] and Zeno APOSTOLIDES[1]

[1] *Department of Biochemistry, Genetics and Microbiology at University of Pretoria, South Africa*

[2] *Department of Anatomy at University of Pretoria, Pretoria, South Africa*

Main/Corresponding Author: Kadima Samuel TSHIYOYO

Master's candidate – Department of Biochemistry, Genetics and Microbiology at University of Pretoria, Private Bag X20, Hatfield, Pretoria, 0028, South Africa

ORCID ID: https://orcid.org/0000-0002-0258-0825

Email: tshiyoyosamuel.ts@gmail.com

Telephone number: +27 79 189 4198

Co-author: Prof Megan Jean BESTER

Professor - Department of Anatomy at University of Pretoria, Pretoria, South Africa

Email: megan.bester@up.ac.za

Co-author: Dr June C. SEREM

Senior lecturer - Department of anatomy at University of Pretoria, Pretoria, South Africa

Email: June.serem@up.ac.za

Co-author: Prof Zeno APOSTOLIDES

Professor - Department of Biochemistry, Genetics, and Microbiology at University of Pretoria, Private Bag X20, Hatfield, Pretoria, 0028, South Africa

Email: zeno.apostolides@up.ac.za

ORCID ID: http://orcid.org/0000-0002-4111-6777

Abstract

Introduction

Several therapeutic targets have been identified for the management of type 2 diabetes (T2D), including the inhibition of α-amylase and α-glucosidase. The present study determined the ability of curcumin, 18α-glycyrrhetinic acid, quercetin and rosmarinic acid to inhibit α-amylase, α-glucosidase, and hepatic lipid accumulation.

Methodology

In-silico enzyme inhibitory abilities of the compounds were assessed using docking analysis with Maestro and AutoDock vina. *In-vitro* biochemical assays were used to confirm docking studies; 3.5-dinitrosalicylic acid (DNSA) and p-nitrophenyl-α-D-glucopyranoside (pNPG) assays for α-amylase and α-glucosidase inhibition, respectively. The ability to reduce lipid accumulation in HepG2 cells for NAFLD was evaluated.

Results

The relationships between *in-silico* and *in-vitro* inhibition results correlated well; a more negative docking score correlated with a lower inhibition constant (K_i). For α-amylase, the K_i values of the compounds were significantly higher ($p < 0.05$) than acarbose. For α-glucosidase, the K_i values of curcumin, 18α-glycyrrhetinic acid (18α-GA), and quercetin were significantly lower ($p < 0.05$) than acarbose. The IC_{50} was determined for these compounds in HepG2 cells. At the concentrations used to evaluate OA-induced lipid accumulation, the compounds were not cytotoxic. All compounds and metformin significantly reduced ($p < 0.05$) lipid accumulation in HepG2 cells.

Conclusion

Herbs/spices are rich sources of these compounds, providing a cost-effective, easily cultivated, and readily available source of compounds that can alleviate T2D symptoms. Curcumin is found in turmeric and rosmarinic acid in rosemary, where a dose of 1.3 g of turmeric or 1.6 g of rosemary is equivalent to 50 mg acarbose per meal.

- **Keywords**

α-amylase, α-glucosidase, herbal compounds, hepatic lipid accumulation, *in-vitro* cytotoxicity, reverse molecular docking, type 2 diabetes.

1. Introduction

Diabetes is a disease associated with hyperglycaemia [1], and develops as a consequence of deficient secretion and/or action of insulin [2]. A recent report from the International Diabetes Federation (IDF) estimated that in 2019, approximately 9.3% of adults worldwide were living with diabetes, and this number could increase to 10.2% and 10.9% in 2030 and 2045, respectively [3]. Type 2 diabetes (T2D) is the most common type of diabetes and accounts for approximately 90-95% of all diabetes patients. Obesity and lack of physical activity are factors associated primarily with T2D [2] and often can lead to other complications, such as non-alcoholic fatty liver disease (NAFLD) [4]. NAFLD is considered to be a major leading cause of liver disease globally and is linked with different factors, such as fatty acid accumulation, insulin resistance, and disruption of insulin sensitivity [4]. The presence of T2D leads to more severe forms of NAFLD while NAFLD contributes to the increased incidence of T2D [5] through increased glucose production and hepatic insulin resistance.

Specific enzymes hydrolyse dietary carbohydrates into monosaccharide before entry into the appropriate cells for energy or storage [6]. The two primary enzymes responsible for the hydrolysis of carbohydrates in the digestive tract [7] are α-amylase and α-glucosidase. α-Amylase is found in saliva and pancreatic juice, and α-glucosidase in the small intestine [8]. These enzymes hydrolyse the α-1,4 glycosidic linkage of oligosaccharides and disaccharides to release glucose into the bloodstream. Pharmacologically, both enzymes are important targets, as enzyme inhibition will delay glucose absorption and consequently reduce the development of hyperglycemia after a meal in T2D patients. Some drugs minimize glucose absorption by inhibiting these enzymes. These inhibitors are acarbose, miglitol, and voglibose [9, 10]. Although all these drugs are currently in use, searching for new potential treatments remains essential due to cost, drug interactions and side effects, such as abdominal pain, fatigue, flatulence and diarrhea [11, 12].

Plants are sources of bioactive compounds that have shown significant benefits in medicine. The different compounds found in plants are mainly phenolics and flavonoids, which have shown to have some therapeutic effects [13]. Some medicinal plants/herbs have been investigated for their ability to help in the management of T2D [14-16]. Several studies have shown that herbal compounds have antidiabetic effects and may cause fewer side effects [12, 19-22].

Curcumin, 18α-GA, rosmarinic acid, and quercetin were the compounds used in the present study, and these compounds have been identified in commercial herbs/spices [14]. Curcumin is a polyphenol found abundantly in turmeric (Curcuma longa) [23]; 18α-GA is a pentacyclic triterpenoid found in liquorice (*Glycyrrhiza glabra*); quercetin is a flavonoid abundantly present in almost all herbs and spices; rosmarinic acid is a phenolic acid found abundantly in rosemary (*Salvia rosmarinus*). The aim of this study was to identify new inhibitors of α-amylase and α-glucosidase using *in-silico* and *in-vitro* studies and to investigate the effects of the compounds on hepatic lipid accumulation.

2. Materials and methods

2.1. Chemicals

The following reagents were obtained from Sigma Aldrich (Missouri, USA): starch, pNPG, acarbose, curcumin, 18α-GA, quercetin, quinic acid, nerolidol, rosmarinic acid, oleic acid, oil red O (ORO), porcine pancreatic α-amylase (EC 3.2.1.1), intestinal α-glucosidase (EC 3.2.1.20) from *Saccharomyces cerevisiae*, 3.5-dinitrosalicylic acid (DNSA), Dulbecco's modified Eagle's medium (DMEM) and sulforhodamine B (SRB). HepG2 hepatocarcinoma cells were purchased from ATCC, and Caco-2 adenocarcinoma cells were obtained from CELLONEX Separation Scientific (Johannesburg, South Africa).

2.2. *In-silico* study

2.2.1. Compound preparation

Chemical structures of the compounds were imported from canvas to Maestro and were drawn as SMILES obtained from PubChem (www.pubchem.ncbi.nlm.nih.gov/). The LigPrep function in Maestro was used to prepare 3D structures from 2D structures, preprocess the structures, and generate multiple poses from each structure [24, 25]. This function ensured that the structures were ready for docking.

2.2.2. Docking software

The *in-silico* data of the compounds were obtained using Maestro and AutoDock Vina from the DIA-DB (http://bio-hpc.eu/software/dia-db/). Maestro is a Schrödinger software that uses the Glide scoring function; this scoring function analyses the different interactions in the ligand–protein complex and minimizes any steric clashes to generate docking scores [26]. AutoDock Vina uses an empirical scoring function that focuses on simple contact terms and the contribution of lipophilic and metal-ligand interactions in the ligand–protein complex to estimate the Gibbs free binding energy between the ligand and the protein [27].

2.2.3. Enzyme preparation

The crystal structures of the enzymes were downloaded to Maestro from the PDB (www.rscb.org) using the respective PDB IDs for pancreatic α-amylase (4GQR) and intestinal α-glucosidase (3L4Y). The protein preparation wizard in Maestro was used to prepare enzymes for molecular docking. All cofactors and water molecules were removed, and the structures were optimized. This wizard resolved structural issues and made the structures suitable for docking (structural-based virtual screening) [25, 28].

2.2.4. Molecular docking

The grid file and the ligand file are needed to run a docking job. The grid file was generated using the receptor grid generation tool in Maestro, keeping the default parameters. Protein docking was performed using glide HTVS, and the prepared ligands were docked against the generated grid file of pancreatic α-amylase and intestinal α-glucosidase enzyme complex. The docking score is relative to the ΔG of the protein-compound interaction; a more negative score indicates stability, thus strong binding affinity of the compound to the protein. Interactions in the protein-compound complex contribute to the estimation of ΔG, including hydrophobic interactions and hydrogen bonds [26, 27].

2.2.5. Physiochemical properties

Selected compounds were further analysed using Schrodinger's canvas program and the online tool pkCSM to obtain pharmacokinetic and toxicity properties. The SMILES notations of the compounds were imported to pkCSM to calculate the physiochemical properties by using a series of databases and machine learning based on learning patterns to build predictive models [29]. This is based on pattern recognition and algorithm to link similarities such between known compounds and possible potential drugs.

2.3. *In-vitro* study

2.3.1. *In-vitro* α-amylase inhibition

To assess the inhibitory activity of the compounds against α-amylase, the following procedure was followed using a colorimetric assay as described by previous literature [30] with modifications. In Eppendorf tubes, 100 µL of the inhibitor (0 to 1.5 mM) was mixed with 100 µL α-amylase (2 U/mL) and

preincubated at approximately 25°C for 10 min before adding 100 µL of substrate starch (0, 2, 4, 5, 6, 8, 9 and 10 mg/mL). After incubation at approximately 25°C for 10 min, 100 µL of DNSA colour reagent (96 mM) was added. After 10-min incubation at 85°C on a heating block, the solution was cooled and diluted with ddH_2O before transferring a 200 µL volume to a 96-well plate, and the absorbance was measured at 540 nm.

2.3.2. *In-vitro* α-glucosidase inhibition

To assess the inhibitory activity of the compounds against α-glucosidase, a colorimetric assay was used following a previous study [30] with slight modifications. Working directly in a 96-well microplate, 50 µL of 0.2 U/mL enzyme in phosphate buffer (100 mM, pH 6.9) and 100 µL of the compound or acarbose (0 to 8 mM) were preincubated at 37°C for 10 min before adding 50 µL of pNPG at different concentrations (0, 0.3, 0.6, 0.8, 1.25, 2.5 and 4 mM) in phosphate buffer (100 mM, pH 6.9). Next, the reaction was incubated at 37°C for 30 min before adding 50 µL of a 1 M NaOH solution. The addition of the base led to the deprotonation of p-nitrophenol, which becomes basic and generates a dark yellow colour that can be read at 405 nm.

2.3.3. *In-vitro* cytotoxicity

The *in* vitro cytotoxicity of the compounds was assessed using the sulforhodamine (SRB) assay. This method was performed similarly to the method used in the following study [31], with slight modifications. In a 96-well plate, a 100 µL cell suspension representing 1×10^5 cells was added to every well and then incubated overnight at 37°C with 5% CO2 to allow cell attachment. A volume of 100 µL compounds in (0.01, 0.1, 1, 10 and 100 µM) was added, and then the plate was incubated at 37°C with 5% CO2 for 72-hours. Wells containing only cells and media were used as the negative control and Saponin was used as the positive control. After the 72-hours incubation period, the cells were fixed with 50 µL of 50% (w/v) trichloroacetic acid solution and incubated overnight at 4°C. The plates were then washed with water and dried in an oven overnight before adding 100 µL of 0.057% w/v SRB solution. After incubation for 30 min, the wells were washed with 1% v/v acetic acid and then dried overnight in an oven. Once dry, 200 µL Tris buffer (10 mM, pH 10.5) was added to each well, followed by gentle shaking at 550 rpm for an hour. The absorbance of the extracted dye was measured at 540 nm, and the IC_{50} representing the concentration that induces 50% cell death was calculated for each compound.

2.3.4. Hepatic lipid accumulation

The effect of the compounds on inhibiting hepatic lipid accumulation was assessed *in-vitro* using the ORO staining method with OA as the stimulant for lipid stimulation. The experiment was carried out according to previous studies [32] [33] with some modifications. HepG2 cells were seeded on 96-well plates at a density of 5×10^4 cells per well and incubated overnight for attachment. The cells were then treated with the compounds and 1 mM OA for 48 hours before fixing the cells with 2% formalin for 30 minutes at 37°C. The medium was discarded, and then 100 µL of the ORO working solution (ratio 3:2 of 0.5% ORO dissolved in H_2O) was added and incubated for 1 hour at room temperature. The staining solution was removed, and the plate was washed with tap water until the water was clear. Then, the plate was blotted dry. Microscopic images were taken to visualize ORO-stained lipid droplets in HepG2 cells. Then, the lipids were extracted with 100 µL of 60% isopropanol solution, and the absorbance was measured at 405 nm. The results are expressed as the percentage lipid accumulation relative to HepG2 cells exposed only to OA using the formula below:

$$\%\ \boldsymbol{lipid\ accumulation} = \frac{(\boldsymbol{Abs.\ test\ sample})}{(\boldsymbol{Abs.\ oleic\ acid\ only})} \times \mathbf{100}\%$$

2.4. Herbs/spices dose-related to acarbose dose

Online databases such as Phenol-Explorer [34] and previous studies, were used to find the amount of each compound in several herbs and spices. The herb or spice with the highest amount of the compound (mg of compound/100 g dry weight of the herb) was used to calculate the dose of each herb related to the dose of acarbose taken per meal, which is 50 mg.

2.5. Statistical analysis

All experiments were performed in triplicate with at least three independent repeats, and the results are expressed as the mean ± standard error of the mean (SEM). Excel from Windows 10 was used to analyse the data before exportation to other software for further analysis. The IC_{50} of the compounds was calculated using GraphPad Prism version 8.3.0 (San Diego, California, USA). Kinetic parameters of the compounds were calculated on Excel from Windows 10, and the graphs were generated using R Studio and Python 3.9. (Delaware, USA) on virtual studio code from Microsoft (Redmond, Washington, USA). The K_i values were obtained from the Lineweaver-Burk plot and by plotting secondary plots, and the data were analysed with a one-sided unpaired Student's t test. Significance was considered at $p<0.05$ and is indicated either with * or a different letter of the English alphabet.

3. Results

3.1. *In-silico* studies

3.1.1. Chemical structures

Many herbs and spices, such as oregano, turmeric, rosemary, and liquorice, are known to have antidiabetic activity [14] [17]. These effects were attributed to the inhibition of carbohydrate hydrolysing enzymes and/or insulin action. Compounds that were the most abundant in these herbs and spices were selected (Figure 1), and these compounds were curcumin, 18α-GA, quercetin and rosmarinic acid with nerolidol and quinic acid as negative controls based on the docking scores. Acarbose a drug widely used in the treatment of T2D was also included as a control.

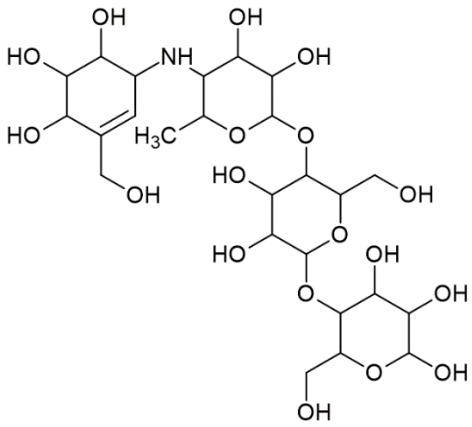

Name: **Acarbose**
Structure: Saccharide

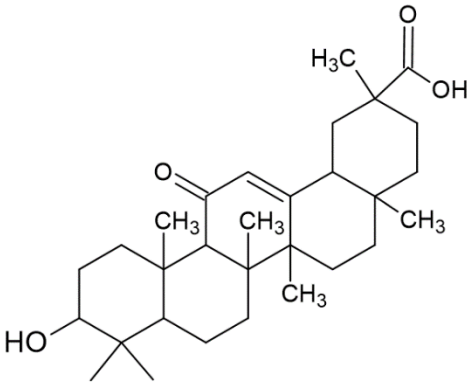

Name: **18α-glycyrrhetinic acid**
Structure: Triterpenoid

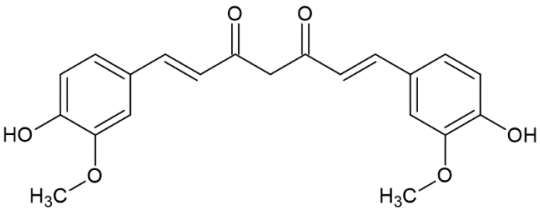

Name: **Curcumin**
Structure: Polyphenol

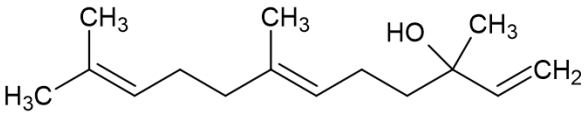

Name: **Nerolidol**
Structure: Terpene

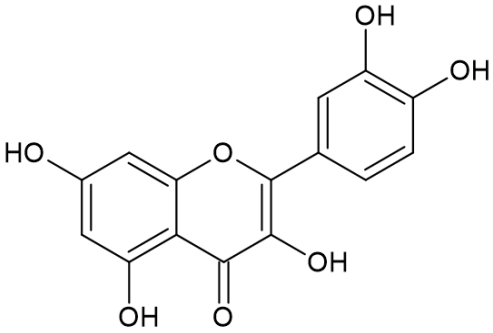

Name: **Quercetin**
Structure: Polyphenol flavonoid

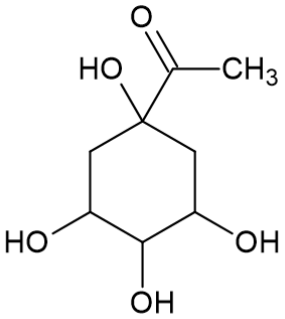

Name: **Quinic acid**
Structure: Cyclitol

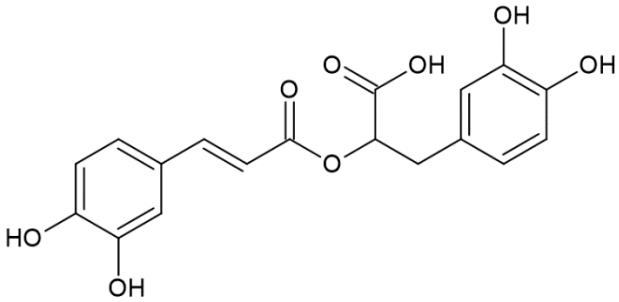

Name: **Rosmarinic acid**
Structure: Phenolic acid

Figure 1. Chemical structures of the selected compounds

3.1.2. Molecular docking

For molecular docking studies, the PDB structures of the human pancreatic α-amylase (PDB ID: 4GQR) and intestinal α-glucosidase (PDB ID: 3LY4) from *Saccharomyces cerevisiae* were used (see Figure S1). Docking was performed using glide functions in Maestro, and the docking scores were then compared to those obtained from DIA-DB using the AutoDock Vina algorithm. The compounds, including acarbose as the positive control, were docked in the active site of both α-amylase and α-glucosidase (see Figures S2 and S3).

***Table 1**. Docking scores of the compounds and acarbose docked to amylase and glucosidase.*

	Docking score (Kcal/mol)			
	α-Amylase		**α-Glucosidase**	
Compound	**Glide**	**AutoDock**	**Glide**	**AutoDock**
Acarbose	-6.5	-7.5	-3.1	-6.5
Curcumin	-6.3	-8.2	-3.3	-7.5
18α-GA	-4.1	-9.8	-2.1	-7.4
Nerolidol	-2.5	-5.9	0.4	-5.9
Quercetin	-6.5	-8.1	-4.6	-7.2
Quinic acid	-5.2	-5.4	-4.7	-4.5
Rosmarinic acid	-6.0	-8.3	-4.1	-7.3

Tables 1 shows the docking scores of the compounds. Curcumin, quercetin and rosmarinic acid had more negative scores than acarbose for α-glucosidase for Maestro and DIA-DB. These compounds were identified as promising compounds for further *in-vitro* studies. On the other hand, nerolidol had a more positive score than acarbose in α-glucosidase for Maestro and DIA-DB; therefore, it was used as a negative control for *in-vitro* studies. Figure 2 shows graphs illustrating the relationship between the two docking algorithm.

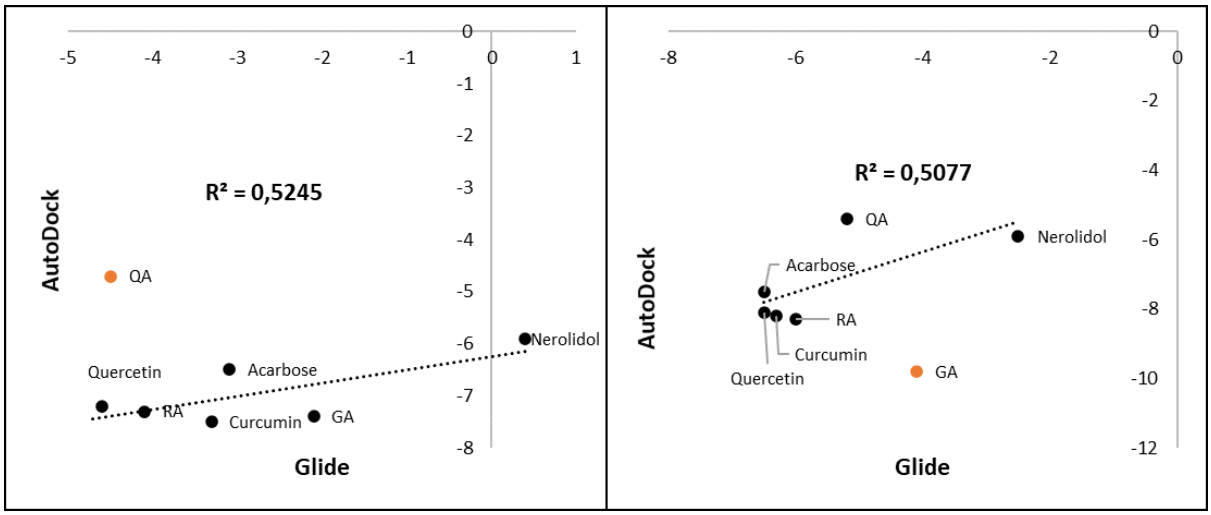

Figure 2. Graph of AutoDock scores vs Glide scores showing the relationship between the Glide and AutoDock docking scores against α -amylase (Right) and α -glucosidase (Left)

***Table 2**. Spearman's and Pearson's correlation coefficients between Glide and AutoDock Vina*

	Spearman's coefficient ρ	**Pearson's coefficient r**
α-Amylase	0.51	0.57

α-Glucosidase	0.46	0.31

Spearman and Pearson's correlation coefficients were used to determine the relationship between the two algorithms; positive coefficients were obtained for the two algorithms in α-amylase and α-glucosidase. A positive coefficient between 0 and 1 indicates a positive relationship between the algorithms in predicting the affinity of the compounds for α-amylase and α-glucosidase (Table 2).

Curcumin, 18α-GA, quercetin, and rosmarinic acid were identified as promising compounds for further analysis based on the positive *in-silico* enzyme docking interactions. In contrast, nerolidol and quinic acid were identified as negative controls due to poor inhibition of both enzymes *in-silico*.

3.1.3. Physiochemical properties

The physiochemical properties of selected compounds were obtained using Canvas a Schrödinger software and pkCSM, and the properties of each compound were compared to acarbose.

Table 3*. Predicted physiochemical properties of acarbose and the compounds*

	HERG inhibitor	**#Stars**	**Bioavailability score**	**Lipinski #violation**
Acarbose	**No**	**13**	**0.17**	**3**
Curcumin	No	0	0.55	0
18α-GA	No	0	0.85	1
Nerolidol	No	2	0.55	0
Quercetin	No	0	0.55	0
Quinic acid	No	0	0.56	0
Rosmarinic acid	No	2	0.56	0

From Table 3, all compounds have a higher bioavailability score than acarbose, indicating that these compounds are absorbed and enter the systemic circulatory system which is not ideal as the targeted enzyme are in the lumen of the small intestine. However, these compounds may be multifunctional and have additional systemic targets. In addition, all the compounds, including acarbose are not inhibitors of the HERG potassium channel. The promising compounds did not violate the Lipinski rules compared to acarbose, which violated three rules. Acarbose had more stars, suggesting that acarbose is less drug-like than compounds with fewer #stars.

3.2. *In-vitro* studies

3.2.1. Kinetics of the *in-vitro* enzyme inhibition

The ability of the compounds to inhibit the enzymes was assessed by determining their K_i values compared to acarbose, the positive control. A lower value indicates more potent enzymatic inhibition.

For α-amylase inhibition (Table 4), the K_i value of acarbose was significantly lower ($p < 0.05$) than the tested compounds. Of the compounds tested, curcumin had the second-lowest K_i value for the inhibition of α-amylase, indicating that it is a more potent inhibitor than the other tested compounds. The mode of inhibition for acarbose, curcumin, 18α-GA, rosmarinic acid, and quinic acid exhibited

mixed-type inhibition. Inhibition by quercetin was competitive, while nerolidol's type inhibition was uncompetitive. Lineweaver burk plot were used to identify the mode of inhibition (Figures S8 and S9).

***Table 4**. K_i values and types of inhibition of amylase by acarbose and the compounds*

Compound	**K_i ± SEM (µM)**	**Type of inhibition**
Acarbose	**31 ± 4**	**Mixed**
Curcumin	154 ± 17[a]	Mixed
Quercetin	465 ± 61[a]	Competitive
18α-glycyrrhetinic acid	723 ± 180[a]	Mixed
Rosmarinic acid	1082 ± 216[a]	Mixed
Quinic acid	2948 ± 169[a]	Mixed
Nerolidol	3044 ± 100[a]	Uncompetitive

Note: [a] Mean values with different letters are significantly different ($p < 0.05$) (n = 3)

***Table 5**. Ki values and types of inhibition of glucosidase by acarbose and the compounds*

Compound	**K_i ± SEM (µM)**	**Type of inhibition**
18α-GA	27 ± 4[b]	Non-competitive
Curcumin	33 ± 2[b]	Mixed
Quercetin	45 ± 6[b]	Mixed
Rosmarinic acid	94 ± 13[a]	Mixed
Acarbose	**130 ± 10[a]**	**Competitive**
Nerolidol	1075 ± 132[c]	Competitive
Quinic acid	2642 ± 394[c]	Competitive

Note: Mean values with different letters are significantly different ($p < 0.05$) (n = 3)

For α-glucosidase inhibition (Table 5), there was a significant difference ($p < 0.05$) between the K_i value of acarbose and those of 18α-GA, curcumin, and quercetin. These values were also significantly lower ($p < 0.05$) than acarbose, suggesting more potent inhibition of α-glucosidase. Only rosmarinic acid had a K_i value not significantly different ($p > 0.05$) from acarbose. The remaining two compounds, nerolidol and quinic acid, had K_i values significantly higher ($p < 0.05$) than acarbose, indicating weaker inhibition of α-glucosidase. The type of inhibition differed. Acarbose, nerolidol and quinic acid exhibited a competitive type of inhibition in which these compounds compete with the substrate pNPG to bind to the active site of α-glucosidase. In contrast, 18α-GA exhibited a non-competitive type of inhibition where binding is at a site other than the active site. Curcumin, quercetin and rosmarinic acid exhibited mixed-type inhibition a mixture of competitive and non-competitive inhibition.

***Table 6**. Spearman's and Pearson's correlation coefficients between in-vitro and in-silico studies for α-amylase and glucosidase*

	Spearman's coefficient ρ		Pearson's coefficient r	
	α-Amylase	**α-Glucosidase**	**α-Amylase**	**α-Glucosidase**
AutoDock	0.32	0.93	0.32	0.93
Glide	0.62	0.43	0.88	0.26

Correlation studies between docking scores and K_i values were conducted by plotting a graph of docking scores (Glide and AutoDock) against the K_i value of each compound. Spearman's and Pearson's correlation coefficients were used to determine the relationship between the two studies. Positive coefficients were obtained for both α-amylase and α-glucosidase. A positive coefficient between 0 and 1 indicates a positive relationship between the *in-vitro* and *in-silico* study of the inhibition of α-amylase and α-glucosidase (Tables 7 and 8).

3.2.2. *In-vitro* cytotoxicity

Cytotoxicity was tested against HepG2 hepatocarcinoma, and Caco-2 adenocarcinoma cells (Table 7). The concentration range used for the evaluation of toxicity included the concentration used for hepatic lipid accumulation. Caco-2 adenocarcinoma cells represent cells of the human intestine and represent the site of α-amylase and α-glucosidase activity.

***Table 7**. IC_{50} (in µM) of acarbose and the compounds on HepG2 and Caco-2 cells*

Compound	**HepG2**	**Caco-2**
Acarbose	> 100	> 100
Curcumin	41 ± 2*	15 ± 1*
18α-GA	28 ± 8*	> 100
Nerolidol	> 100	> 100
Quercetin	54 ± 2*	> 100
Quinic acid	> 100	> 100
Rosmarinic acid	> 100	83 ± 3*

In the HepG2 cell line, 18α-GA, curcumin, and quercetin had significantly lower ($p < 0.05$) IC_{50} values than acarbose. In contrast, no cytotoxicity in this cell line was observed for rosmarinic acid, quinic acid and nerolidol at concentrations up to 100 µM.

In the Caco-2 cell line, the IC_{50} of curcumin and rosmarinic acid was significantly lower than the IC_{50} of acarbose. Quercetin, nerolidol, quinic acid and 18α-GA were not cytotoxic at any of the concentrations evaluated.

3.2.3. Hepatic lipid accumulation

Oleic acid induces lipid droplet accumulation in HepG2 cells, treatment with the compounds were compared to the control with OA added and the vehicle control (DMSO) with no OA added after 48

hours exposure (Figure 3). Quantification of lipid droplets after treatment with metformin at 1 and 10 µM indicated a significant decrease in lipid accumulation (Figure 3). At 1 µM, curcumin, quercetin, and quinic acid caused a significant decrease in lipid accumulation. At 10 µM, all compounds except curcumin caused a significant decrease in lipid accumulation. Metformin and quercetin showed a significant dose-dependent decrease in lipid accumulation. 18α-GA and rosmarinic acid at 10 µM induced the greatest decrease in lipid droplet accumulation compared with the other compounds.

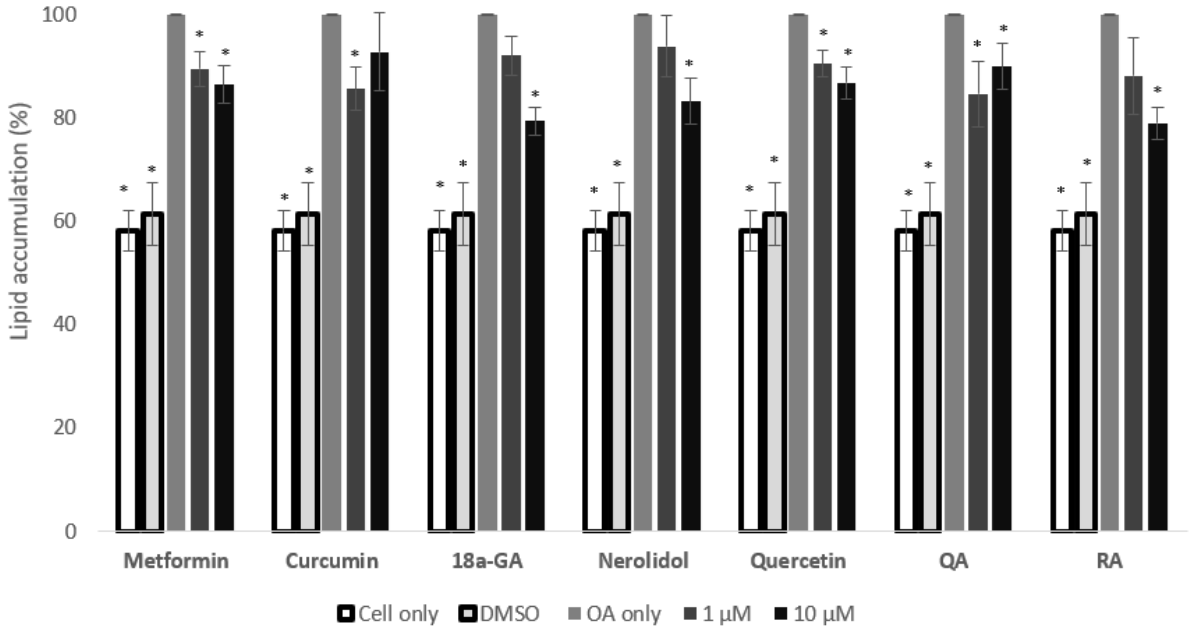

*Figure 3. Lipid accumulation in HepG2 cells. Cells were exposed for 48 hrs to oleic acid (OA) only or a combination of OA and 1 and 10 µM of the following compounds: metformin (control), curcumin, 18α-GA, (GA), nerolidol, quercetin, quinic acid (QA) and rosmarinic acid (RA). Data are represented as Mean ± SEM. * $p < 0.05$ compared to OA only treatment.*

Microscopic images (Figure 4) show the lack of ORO staining for the vehicle control, which contrasts with the red staining observed for cells exposed to OA. Although some staining was observed for all cells exposed to OA in combination with the tested compounds, the intensity of staining was reduced and was confirmed following the extraction of ORO (Figure 4).

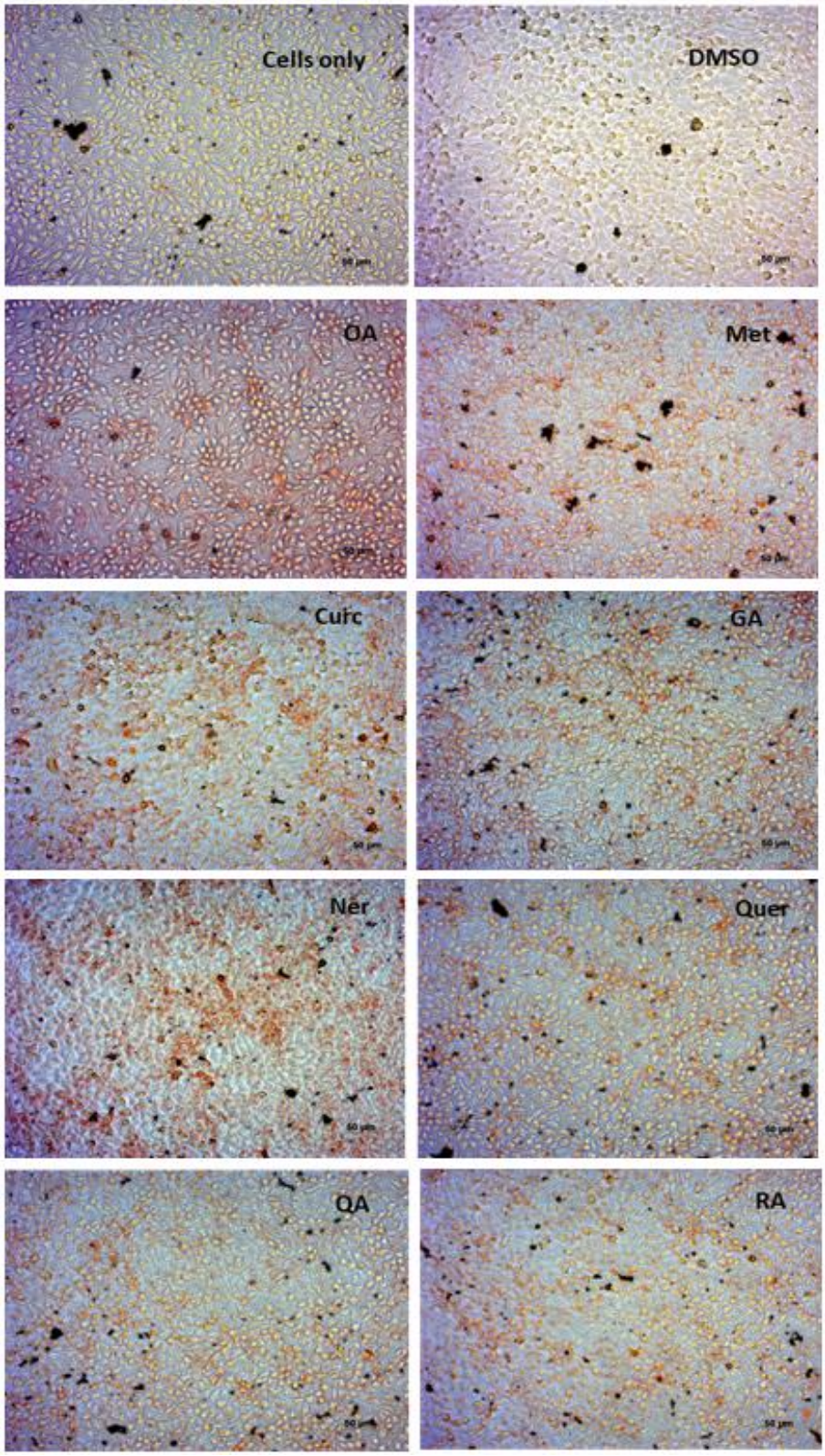

Figure 4. Light microscopy images showing the lipid accumulation in HepG2 cells after staining with Oil Red O solution. The controls were HepG2 cells alone and exposed to DMSO, (vehicle control), oleic acid (OA) (positive control) and 10 µM metformin (Met), curcumin (Curc), 18α-GA (GA), nerolidol (Ner), quercetin (Quer), quinic acid (QA) and rosmarinic acid (RA). Images were captured at 40 x original magnification.

3.3. Herbs/spices dose-related to acarbose dose

The herbs and spices with the highest contents of curcumin, glycyrrhizin, quercetin, quinic acid and rosmarinic acid were identified from previous studies and their equivalent relating to acarbose per meal was calculated. Table 18 is showing a small amount of Turmeric, 1.3 g dry weight may be required to match the dose of acarbose per meal. Green tea, Peppermint and Rosemary have also shown small amount, 1.9, 1.6, and 1.8 g dry weight, respectively. This relates to the moles of selected compounds to approximately match the moles in the dose of acarbose per meal.

***Table 8**. Herb/spice dosage required relative to acarbose*

Compound	**Herb or spice (Species)**	**Amount in herb/spice (mg/100 g dry weight)**	**Amount (g) of herb relative to acarbose per meal**
Curcumin	Turmeric (*Curcuma longa*)	2213	1.30
	Curry powder (*Murraya koenigii*)	285	10.0
Glycyrrhizin	Liquorice (*Glycyrrhiza glabra*)	239	27.0
Quercetin	Oregano (*Lippia graveleones*)	42.0	56.0
	Green tea (*Camelia sinensis*)	2.80	845
Quinic acid	Green tea (*Camelia sinensis*)	795	1.90
Rosmarinic acid	Peppermint (*Mentha piperita*)	1620	1.60
	Rosemary (*Salvia rosmarinus*)	1534	1.80

Curcumin and rosmarinic acid, which are potent inhibitors of α-glucosidase and reduce hepatic lipid accumulation, were present in turmeric as well as peppermint and rosemary, respectively. These results indicate that these herbs have antidiabetic properties.

4. Discussion

In-silico studies were used as a step in the selection of the compounds to be used. Compounds were selected based on the docking scores compared with acarbose. The compounds were docked in the active site of α-amylase and α-glucosidase to generate binding energy (ΔG), where a more negative binding energy indicates a spontaneous interaction and a stronger affinity between the ligand and protein, thus more potent inhibition.

For pancreatic α-amylase *in-silico* inhibition (Table 1), the order of affinity was as follows: acarbose > quercetin > curcumin > rosmarinic acid > quinic acid > 18α-GA > nerolidol when docked with glide; and 18α-GA > rosmarinic acid > curcumin > quercetin > acarbose > nerolidol > quinic acid when docked with AutoDock vina. Compared to acarbose, curcumin, 18α-GA, quercetin, and rosmarinic acid are considered potential inhibitors of α-amylase and α-glucosidase. Nerolidol was considered to be a weak inhibitor of both enzymes.

For α-glucosidase *in-silico* inhibition (Table 1), the order of affinity was as follows: quinic acid > quercetin > rosmarinic acid > curcumin > acarbose > 18α-GA > nerolidol when docked with glide; and curcumin > 18α-GA > rosmarinic acid > quercetin > acarbose > nerolidol > quinic acid when docked with AutoDock vina. Similar to these findings, Jhong et al. [37] reported a higher *in-silico* binding affinity to α-glucosidase for curcumin with docking scores more negative than acarbose. However, they used PDB ID 2ZE0 while we used PDB ID 3L4Y, and the authors used AutoDock for their scoring function. A study by Tolmie et al. [30] reported that rosmarinic acid has a higher *in-silico* binding affinity to α-glucosidase than acarbose, and as in the present study, the same PDB ID and the glide algorithm were used. These results were used as motivation to perform *in-vitro* enzyme inhibition to further investigate the potential inhibitory activities of these compounds against pancreatic α-amylase and intestinal α-glucosidase.

For systemic applications, it is important to determine the ADMET properties of the compounds. This was generated *in-silico* using Schrödinger software known as QikProp and an online free tool, pkCSM. All compounds, including acarbose, were predicted not to be inhibitors of the HERG potassium (K^+) channel.

A bioavailability score close to 1 indicates that these drugs are absorbed into the circulation before reaching their target [38]. The bioavailability of the compounds was assessed and compared to acarbose, which mediates its effect in the gastrointestinal tract and had a lower bioavailability score of 0.17. 18α-GA had the highest bioavailability score of 0.85. Curcumin, nerolidol, quercetin, quinic acid, and rosmarinic acid had a bioavailability score of 0.5, showing that almost half of these compounds are absorbed into the circulation. The target enzymes are located at the lumen of the small intestine; hence it is important to have a lower bioavailability score indicating that more of the compound remained at the target site. However, if absorbed, these compounds may well have systemic targets and as multifunctional molecules preventing T2D.

The Lipinski rule of five is used to determine the parameters associated with 90% of orally administered drugs that have passed the phase II clinical stage trial [40, 41]. The results from Table 3 show that acarbose violated three rules, while the remaining compounds did not violate more than one of five rules.

The inhibitory concentrations of the compounds were obtained from Lineweaver-Burk double reciprocal plots and secondary plots. None of the selected compounds showed stronger *in-vitro* inhibition of pancreatic α-amylase than acarbose. The increasing order of K_i values was as follows (Table 4): acarbose < curcumin < quercetin < 18α-GA < rosmarinic acid < quinic acid < nerolidol. Like in the present study, Jhong et al. [37] showed that curcumin more potently inhibited pancreatic α-amylase than quercetin, with the IC_{50} of curcumin being lower than that of quercetin. In the latter study, curcumin and quercetin more potently inhibited pancreatic α-amylase than acarbose, with IC_{50} values being lower than that of acarbose. Although some compounds showed mild inhibition of α-amylase, this may be preferred, as it may help prevent excessive bacterial fermentation that can lead to adverse gastrointestinal side effects [30, 42].

The increasing order of the K_i values in the inhibition of α-glucosidase was as follows: 18α-GA < curcumin < quercetin < rosmarinic acid < acarbose < nerolidol < quinic acid (Table 5). The compounds 18α-GA, curcumin, and quercetin showed stronger in vitro inhibition of α-glucosidase than acarbose, the positive control. In contrast, the efficacy of rosmarinic acid was similar to that of acarbose for the inhibition of α-glucosidase, with a K_i value not significantly different ($p > 0.05$). Jhong et al. [37] also reported more potent inhibition of α-glucosidase by curcumin and quercetin compared to acarbose. In this study, the IC_{50} values were used for comparison, with the IC_{50} values of curcumin and quercetin

being lower than that of acarbose. No data have previously been reported for the inhibition of α-glucosidase by 18α-GA, although Ko et al. [43] reported some antidiabetic properties for 18α-GA related to insulin-stimulated glucose uptake in adipocytes.

Cytotoxicity in the Caco-2 cells was used to predict the effect of the tested compounds in the small intestine where both carbohydrate hydrolysing enzymes are located. For curcumin and rosmarinic acid, IC_{50} values of 15 and 83 µM, respectively, could be determined, while for the remaining compounds at the highest concentration of 100 µM, 50% toxicity could not be determined. A study by Sueki et al. [44] showed that Caco-2 cells are more resistive to curcumin, where at 50 µM, only 16.2% toxicity was observed in Caco-2 cells after 24 hours of exposure.

Rosmarinic acid, acarbose, quinic acid, and nerolidol were not cytotoxic in the HepG2 cell line. The IC_{50} values for 18α-GA > curcumin > quercetin was 28 ± 8, 41± 2, 54 ± 2 µM, respectively. This confirms the findings of Tolmie et al. [30], who reported limited toxicity in the same cell line even at concentrations as high as 500 µM.

The different cell lines responded differently to the compounds and may be related to the doubling times and cellular metabolism related to cellular ADMET, with HepG2 cells being more sensitive than Caco-2 cells. For the lipid accumulation studies, the HepG2 cells were exposed to 10 µM of the compounds for 48 hours, where these compounds would have limited toxicity. Microscopy images of HepG2 cells exposed to OA and the compounds also show the lack of cellular features associated with toxicity.

Metformin and the compounds evaluated significantly decreased OA-induced lipid accumulation in HepG2 cells. No significant difference was observed between the promising compounds and metformin. Rosmarinic acid caused the highest decrease in hepatic lipid accumulation at 10 µM compared with the other compounds. A study by Balachander et al. [47] showed a similar result to the present study, where both rosmarinic acid and metformin significantly reduced OA-induced lipid accumulation in HepG2 cells and can be considered potential compounds in the management of NAFLD. Curcumin reduced lipid accumulation in OA-induced HepG2 cells after 24 hours of exposure [48]. Likewise, previous studies [49, 50] also found a reduction in hepatic OA-induced lipid accumulation by quercetin, and the proposed mechanisms were the downregulation of the levels of sterol regulatory element-binding protein-1c (SREBP-1c) and the enhancement of tyrosine phosphorylation which are important signals in fat accumulation.

In the present study, the promising compounds improved hepatic lipid accumulation and can be used as a potential treatment in NAFLD by decreasing OA-induced lipid accumulation while also taking into consideration the bioavailability scores. The present study confirms the findings of previous studies for curcumin, rosmarinic acid and quercetin, but the beneficial effects of 18α-GA, quinic acid and nerolidol have not yet been reported.

Several different herbs and spices can be a source of these compounds, and screening of herbs and spices identified turmeric as a rich source of curcumin and rosemary as a rich source of rosmarinic acid. Including herbs or spices in the diet may be beneficial.

5. Conclusion

With the increased prevalence of diabetes and its effect on NAFLD, a search for natural compounds to manage hyperglycemia is ongoing. In the present study, compounds found in commercially available herbs and spices are reported to possess antidiabetic activities with the ability to inhibit α-amylase and α-glucosidase. To determine the potential activity of the selected compounds, *in-silico*

and *in-vitro* studies were conducted and compared. The two studies correlated well with positive Pearson and Spearman correlation coefficients. The results showed that curcumin, 18α-GA, quercetin, and rosmarinic acid inhibited α-glucosidase well and decreased hepatic lipid accumulation, indicating the potential of these compounds to alleviate prolonged hyperglycemia and potentially manage NAFLD. Many of these compounds are found in herbs and spices that are cost-effective, easily cultivated, and readily available. Related to the levels of curcumin in turmeric and rosmarinic acid in rosemary, a dose of 1.3 g and 1.6 g dry weight of turmeric and rosemary respectively, are equivalent to 50 mg acarbose per meal. Furthermore, synergism between compounds may have further beneficial effects, and future research can focus on these aspects.

- **Acknowledgment and funding**

This work was based on the research supported by the National Research Foundation (NRF) of South Africa (Grant Numbers: 46712)".

References

1. Egan, A.M. and S.F. Dinneen, *What is diabetes?* Medicine, 2019. **47**(1): p. 1-4.
2. Association, A.D., *Diagnosis and classification of diabetes mellitus.* Diabetes care, 2014. **37**(Supplement 1): p. S81-S90.
3. IDF, I.D.F., *Diabetes atlas*, in *International Diabetes Federation*. 2019: Brussels.
4. Pei, K., et al., *An overview of lipid metabolism and nonalcoholic fatty liver disease.* BioMed Research International, 2020. **40:** p.249-261.
5. Xia, M.-F., H. Bian, and X. Gao, *NAFLD and Diabetes: Two Sides of the Same Coin? Rationale for Gene-Based Personalized NAFLD Treatment.* Frontiers in Pharmacology, 2019. **877**(10), p. 3889-3400.
6. Adefegha, A., et al., *Inhibitory effects of aqueous extract of two varieties of ginger on some key enzymes linked to type-2 diabetes in-vitro.* Journal of Food and Nutrition Research, 2010. **49**(1): p. 14-20.
7. Bhandari, M.R., et al., *α-Glucosidase and α-amylase inhibitory activities of Nepalese medicinal herb Pakhanbhed (Bergenia ciliata, Haw.).* Food Chemistry, 2008. **106**(1): p. 247-252.
8. Zhang, J., et al., *A colorimetric method for α-glucosidase activity assay and its inhibitor screening based on aggregation of gold nanoparticles induced by specific recognition between phenylenediboronic acid and 4-aminophenyl-α-d-glucopyranoside.* Nano Research, 2015. **8**(3): p. 920-930.
9. Kahn, S.E., M.E. Cooper, and S. Del Prato, *Pathophysiology and treatment of type 2 diabetes: perspectives on the past, present, and future.* The Lancet, 2014. **383**(9922): p. 1068-1083.
10. Jayaraj, S., S. Suresh, and R.K. Kadeppagari, *Amylase inhibitors and their biomedical applications.* Starch-Stärke, 2013. **65**(7-8): p. 535-542.
11. Turner, N., et al., *Repurposing drugs to target the diabetes epidemic.* Trends in Pharmacological Sciences, 2016. **37**(5): p. 379-389.
12. Proença, C., et al., *Evaluation of a flavonoids library for inhibition of pancreatic α-amylase towards a structure–activity relationship.* Journal of Enzyme Inhibition and Medicinal Chemistry, 2019. **34**(1): p. 577-588.
13. Murevanhema, Y.Y., V.A. Jideani, and O.O. Oguntibeju, *Review on potential of seeds and value-added products of Bambara groundnut (Vigna subterranea): antioxidant, anti-Inflammatory, and anti-oxidative stress*, in *bioactive compounds of medicinal plants*. 2018, Apple Academic Press. p. 141-188.
14. Pereira, A.S., et al., *Evaluation of the anti-diabetic activity of some common herbs and spices: Providing new insights with inverse virtual screening.* Molecules, 2019. **24**(22): p. 4030-4072.
15. Christensen, K.B., et al., *Identification of plant extracts with potential antidiabetic properties: effect on human peroxisome proliferator-activated receptor (PPAR), adipocyte differentiation and insulin-stimulated glucose uptake.* Phytotherapy Research: An International Journal Devoted to Pharmacological and Toxicological Evaluation of Natural Product Derivatives, 2009. **23**(9): p. 1316-1325.
16. Khacheba, I., A. Djeridane, and M. Yousfi, *Twenty traditional Algerian plants used in diabetes therapy as strong inhibitors of α-amylase activity.* International Journal of Carbohydrate Chemistry, 2014. **28**(72), 81-93.
17. El-Sayed, S.M. and A.M. Youssef, *Potential application of herbs and spices and their effects in functional dairy products.* Heliyon, 2019. **5**(6): p. e01989.
18. Srinivasan, K., *Plant foods in the management of diabetes mellitus: spices as beneficial antidiabetic food adjuncts.* International Journal of Food Sciences and Nutrition, 2005. **56**(6): p. 399-414.
19. Naimi, M., et al., *Rosemary extract as a potential anti-hyperglycemic agent: current evidence and future perspectives.* Nutrients, 2017. **9**(9): p. 968-987.

20. Adelakun, O.E., I.F. Bolarinwa, and J.A. Adejuyitan, *Bioactive compounds in plants and their antioxidant capacity*, in *bioactive compounds of medicinal plants*. 2018, Apple Academic Press. p. 53-74.
21. Xu, H., *Inhibition kinetics of flavonoids on yeast α-glucosidase merged with docking simulations.* Protein and Peptide Letters, 2010. **17**(10): p. 1270-1279.
22. Şöhretoğlu, D., et al., *Discovery of potent α-glucosidase inhibitor flavonols: Insights into mechanism of action through inhibition kinetics and docking simulations.* Bioorganic Chemistry, 2018. **79**: p. 257-264.
23. Goel, A., A.B. Kunnumakkara, and B.B. Aggarwal, *Curcumin as "Curecumin": from kitchen to clinic.* Biochemical pharmacology, 2008. **75**(4): p. 787-809.
24. Gadakar, P.K., et al., *Pose prediction accuracy in docking studies and enrichment of actives in the active site of GSK-3β.* Journal of chemical information and modeling, 2007. **47**(4): p. 1446-1459.
25. Madhavi Sastry, G., et al., *Protein and ligand preparation: parameters, protocols, and influence on virtual screening enrichments.* Journal of Computer-Aided Molecular Design, 2013. **27**(3): p. 221-234.
26. Friesner, R.A., et al., *Glide: a new approach for rapid, accurate docking and scoring. 1. Method and assessment of docking accuracy.* Journal of Medicinal Chemistry, 2004. **47**(7): p. 1739-1749.
27. Eldridge, M.D., et al., *Empirical scoring functions: The development of a fast empirical scoring function to estimate the binding affinity of ligands in receptor complexes.* Journal of Computer-Aided Molecular Design, 1997. **11**(5): p. 425-445.
28. Schrodinger, *Glide 6.7 User Manual*. 2015: Schrodinger Press.
29. Pires, D.E., T.L. Blundell, and D.B. Ascher, *pkCSM: predicting small-molecule pharmacokinetic and toxicity properties using graph-based signatures.* Journal of Medicinal Chemistry, 2015. **58**(9): p. 4066-4072.
30. Tolmie, M., M.J. Bester, and Z. Apostolides, *Inhibition of α-glucosidase and α-amylase by herbal compounds for the treatment of type 2 diabetes: A validation of in-silico reverse docking with in-vitro enzyme assays.* Journal of Diabetes, 2021. **13**(10), p. 779-791.
31. Vichai, V. and K. Kirtikara, *Sulforhodamine B colorimetric assay for cytotoxicity screening.* Nature Protocols, 2006. **1**(3): p. 1112-1116.
32. Huang, W.-C., et al., *Ginkgolide C reduced oleic acid-induced lipid accumulation in HepG2 cells.* Saudi Pharmaceutical Journal, 2018. **26**(8): p. 1178-1184.
33. Theerakittayakorn, K. and T. Bunprasert, *Differentiation capacity of mouse L929 fibroblastic cell line compare with human dermal fibroblast.* World Academy of Science, Engineering and Technology International Journal of Medical and Health Sciences, 2011. **5**(51): p. 373-376.
34. Neveu, V., et al., *Phenol-Explorer: an online comprehensive database on polyphenol contents in foods.* Database, 2010. **40**(1), 1207-1215.
35. Tian, M., H. Yan, and K.H. Row, *Extraction of glycyrrhizic acid and glabridin from licorice.* International Journal of Molecular Sciences, 2008. **9**(4): p. 571-577.
36. Li, J.-y., et al., *Glycyrrhizic acid in the treatment of liver diseases: literature review.* BioMed Research International, 2014. **87**(21), 39-54.
37. Jhong, C.H., et al., *Screening alpha-glucosidase and alpha-amylase inhibitors from natural compounds by molecular docking in-silico.* Biofactors, 2015. **41**(4): p. 242-251.
38. Ntie-Kang, F., *An in-silico evaluation of the ADMET profile of the StreptomeDB database.* SpringerPlus, 2013. **2**(1): p. 1-11.
39. Schrodinger, *QikProp 3.5 user manual*. 2012: Schrodinger press.
40. Lipinski, C.A., et al., *Experimental and computational approaches to estimate solubility and permeability in drug discovery and development settings.* Advanced Drug Delivery Reviews, 1997. **23**(1-3): p. 3-25.

41. Lipinski, C.A., *Lead-and drug-like compounds: the rule-of-five revolution.* Drug Discovery Today: Technologies, 2004. **1**(4): p. 337-341.
42. Etxeberria, U., et al., *Antidiabetic effects of natural plant extracts via inhibition of carbohydrate hydrolysis enzymes with emphasis on pancreatic alpha amylase.* Expert Opinion on Therapeutic Targets, 2012. **16**(3): p. 269-297.
43. Ko, B.-S., et al., *Changes in components, glycyrrhizin and glycyrrhetinic acid, in raw Glycyrrhiza uralensis Fisch, modify insulin sensitizing and insulinotropic actions.* Bioscience, Biotechnology, and Biochemistry, 2007: p. 0705080394-0705080394.
44. Şueki, F., M.K. Ruhi, and M. Gülsoy, *The effect of curcumin in antitumor photodynamic therapy: in-vitro experiments with Caco-2 and PC-3 cancer lines.* Photodiagnosis and Photodynamic Therapy, 2019. **27**: p. 95-99.
45. Chen, C., et al., *Effect of quercetin on dexamethasone-induced C2C12 skeletal muscle cell injury.* Molecules, 2020. **25**(14): p. 3267.
46. Septisetyani, E., et al. *Cytotoxic effects of chemopreventive agents curcumin, naringin and epigallocathecin-3-gallate in C2C12 myoblast cells*. in *IOP Conference Series: Earth and Environmental Science*. IOP Publishing, 2020. **439**, 62-69.
47. Balachander, G.J., S. Subramanian, and K. Ilango, *Rosmarinic acid attenuates hepatic steatosis by modulating ER stress and autophagy in oleic acid-induced HepG2 cells.* RSC advances, 2018. **8**(47): p. 26656-26663.
48. Kang, O., et al., *Curcumin decreases oleic acid-induced lipid accumulation via AMPK phosphorylation in hepatocarcinoma cells.* European Review for Medical and Pharmacological Science, 2013. **17**(19): p. 2578-2586.
49. Li, X., et al., *Quercetin improves insulin resistance and hepatic lipid accumulation in-vitro in a NAFLD cell model.* Biomedical Reports, 2013. **1**(1): p. 71-76.
50. Vidyashankar, S., R.S. Varma, and P.S. Patki, *Quercetin ameliorate insulin resistance and up-regulates cellular antioxidants during oleic acid induced hepatic steatosis in HepG2 cells.* Toxicology In Vitro, 2013. **27**(2): p. 945-953.